Supporting Information

Novel antimicrobial polyglycidols: relationship between structure and properties

Fabian Marquardt, Cornelia Stöcker, Rita Gartzen, Elisabeth Heine, Helmut Keul*, Martin Möller*

Institute of Technical and Macromolecular Chemistry, RWTH Aachen University and DWI-Leibniz-Institute for Interactive Materials, Forckenbeckstr. 50, D-52056 Aachen, Germany; Marquardt@dwi.rwth-aachen.de (F. M.); Cornelia.stoecker@rwth-aachen.de (C. S.); Gartzen@dwi.rwth-aachen.de (R. G.); Heine@dwi.rwth-aachen.de (E. H.)
* Correspondence: Keul@dwi.rwth-aachen.de (H. K.); Moeller@dwi.rwth-aachen.de (M. M.)

1. Synthesis of linear polyglycidol (1)

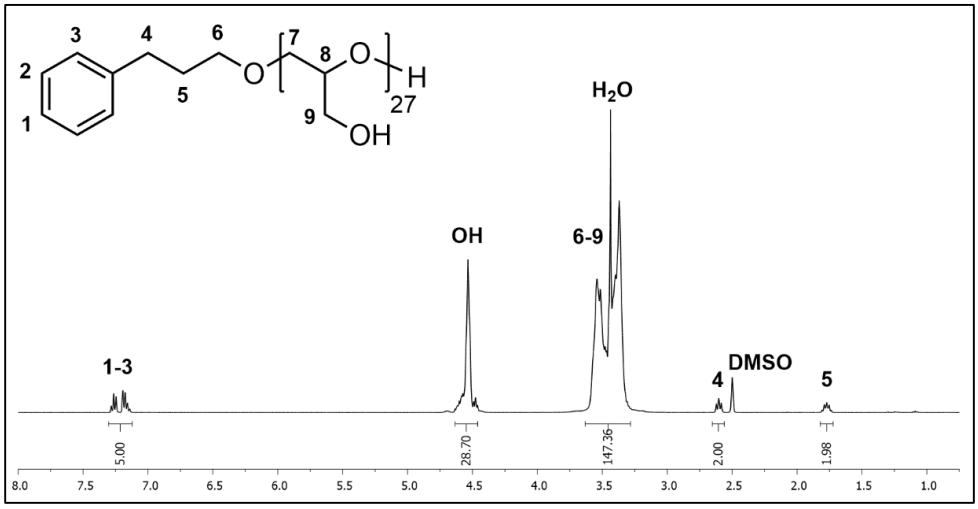

Figure S1. ^{1}H NMR spectrum of PG$_{27}$ (**1**) measured in DMSO-d_6.

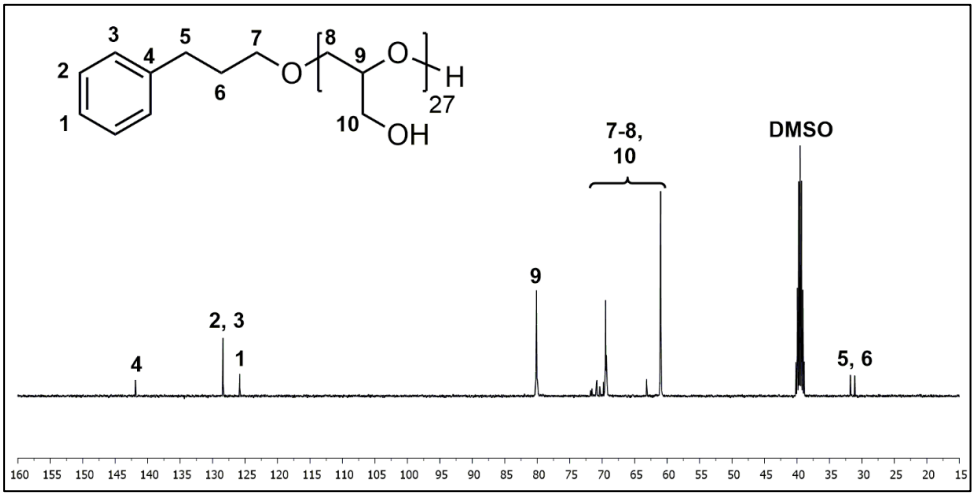

Figure S2. ^{13}C NMR spectrum of PG$_{27}$ (**1**) measured in DMSO-d_6.

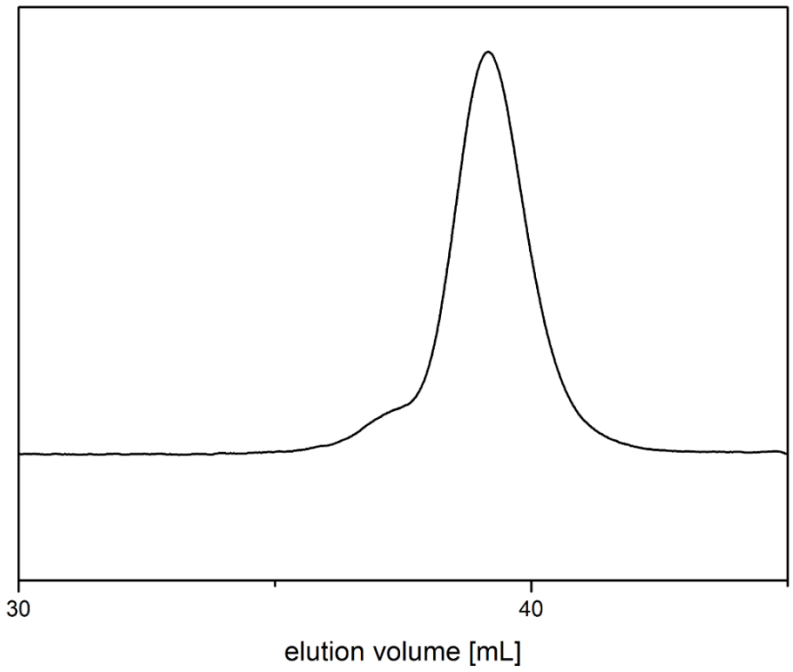

Figure S3. DMF-SEC traces of PG_{27} (**1**).

2. Synthetic pathway

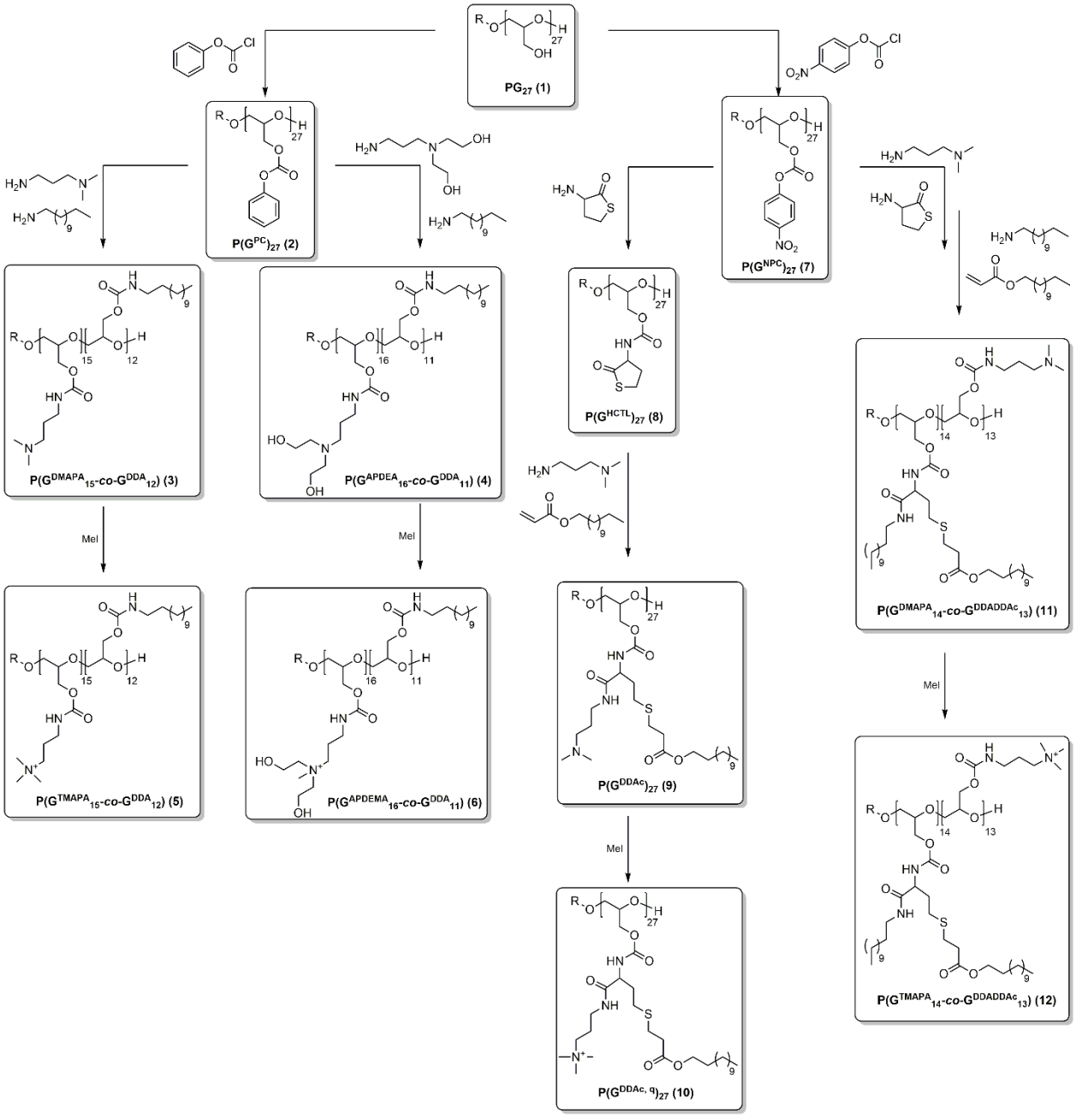

Scheme S1: Synthetic pathway to P(G^{TMAPA}_{15}-*co*-G^{DDA}_{12}) (**5**), P(G^{APDEMA}_{16}-*co*-G^{DDA}_{11}) (**6**), P($G^{DDAc,\ q}$)$_{27}$ (**10**) and P(G^{TMAPA}_{14}-*co*-$G^{DDADDAc}_{13}$) (**12**).

3. Synthesis of P(G$^{TMAPA}_{15}$-*co*-G$^{DDA}_{12}$) (5) and P(G$^{APDEMA}_{16}$-*co*-G$^{DDA}_{11}$) (6)

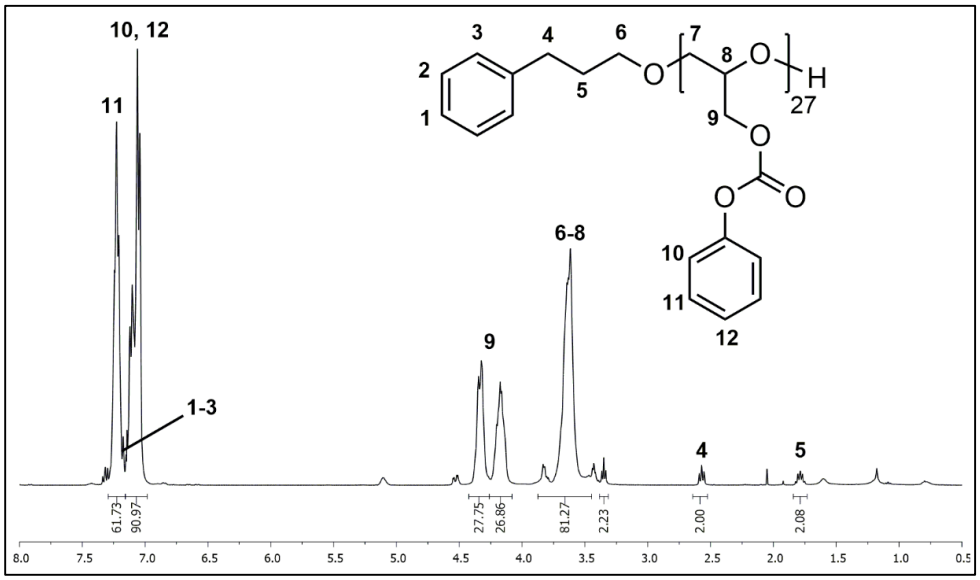

Figure S4. ^{1}H NMR spectrum of P(G^{PC})$_{27}$ (**2**) measured in CDCl$_3$.

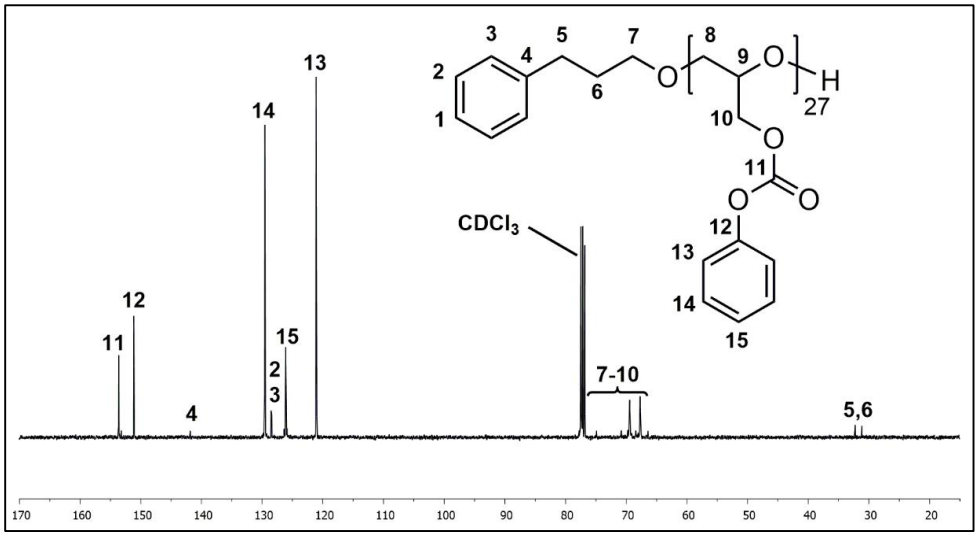

Figure S5. ^{13}C NMR spectrum of P(G^{PC})$_{27}$ (**2**) measured in CDCl$_3$.

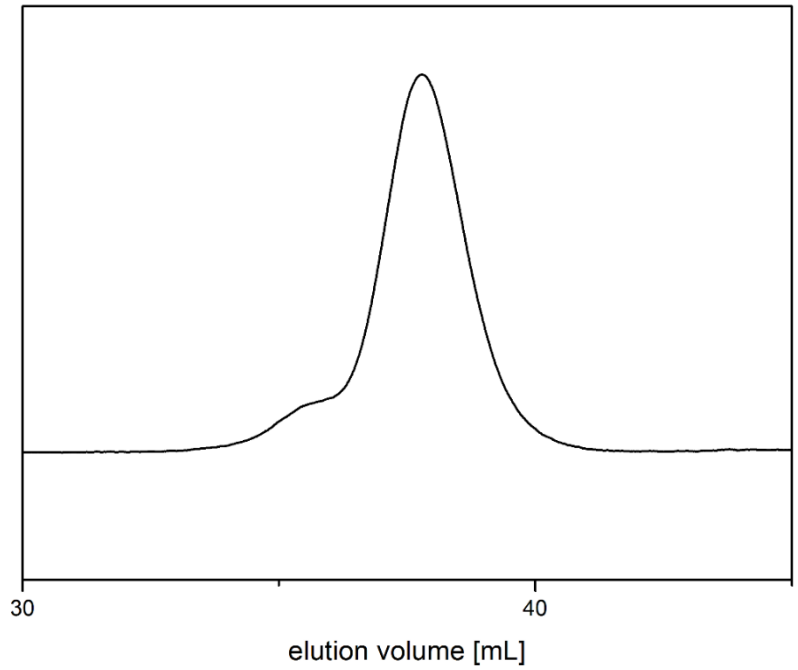

Figure S6. DMF-SEC traces of P(G^{PC})$_{27}$ (**2**).

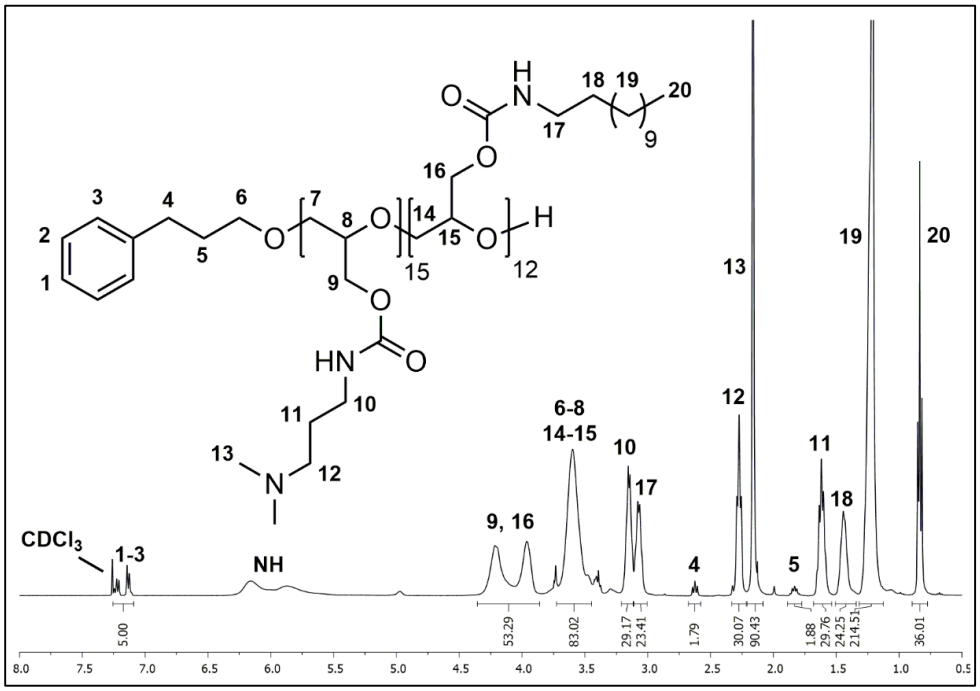

Figure S7. ^{1}H NMR spectrum of P(G^{DMAPA}_{15}-*co*-G^{DDA}_{12}) (**3**) measured in $CDCl_3$.

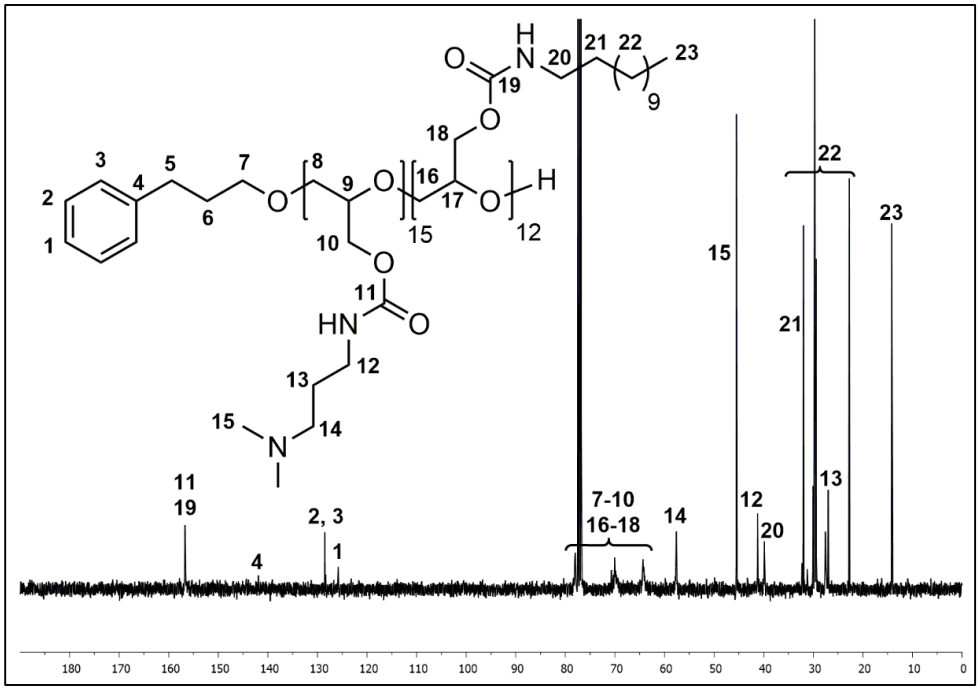

Figure S8. ^{13}C NMR spectrum of P(G^{DMAPA}_{15}-*co*-G^{DDA}_{12}) (**3**) measured in $CDCl_3$.

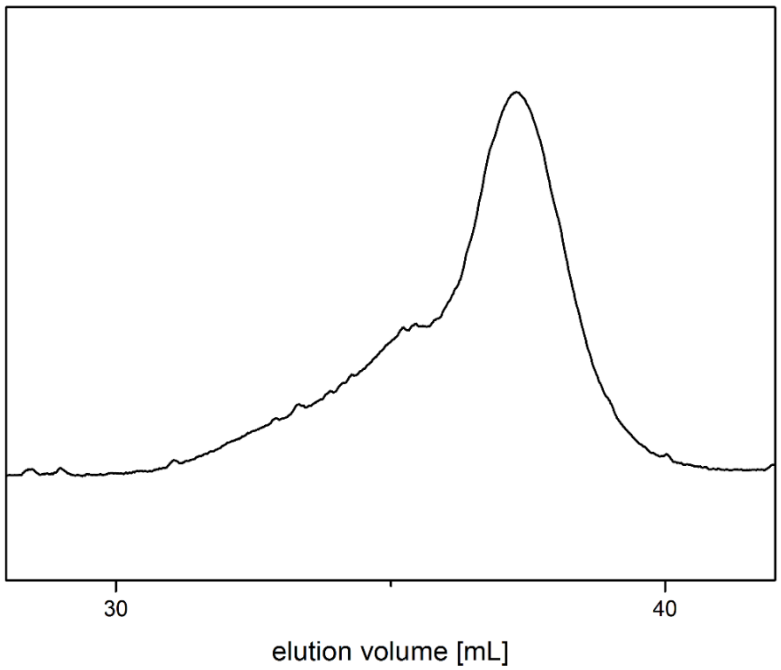

Figure S9. DMF-SEC traces of P(G^{DMAPA}_{15}-*co*-G^{DDA}_{12}) (**3**).

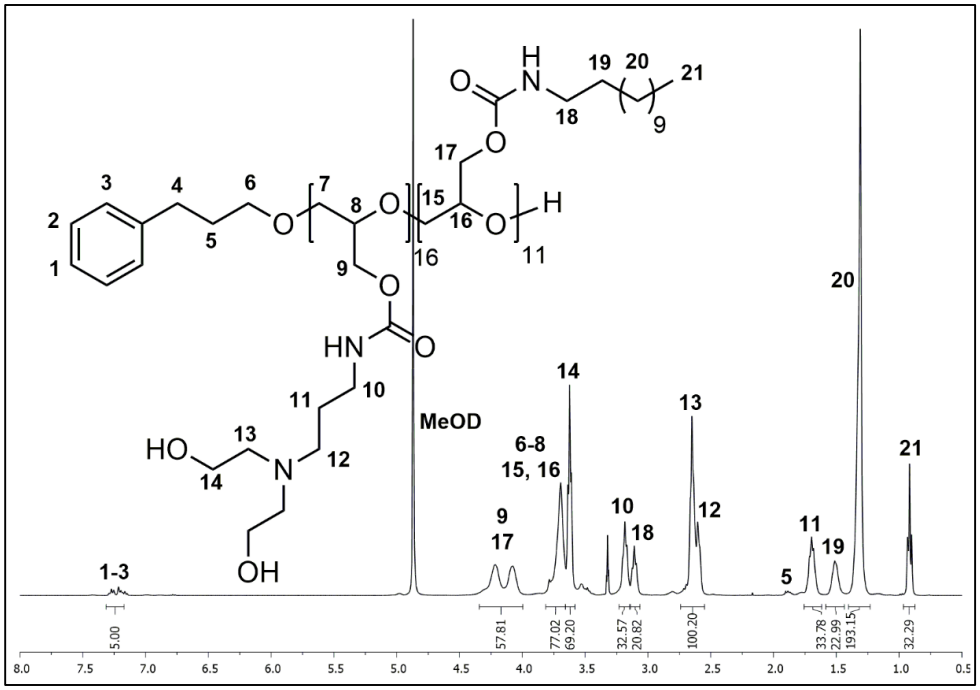

Figure S10. ^{1}H NMR spectrum of P(G$^{APDEA}_{16}$-*co*-G$^{DDA}_{11}$) (**4**) measured in MeOD.

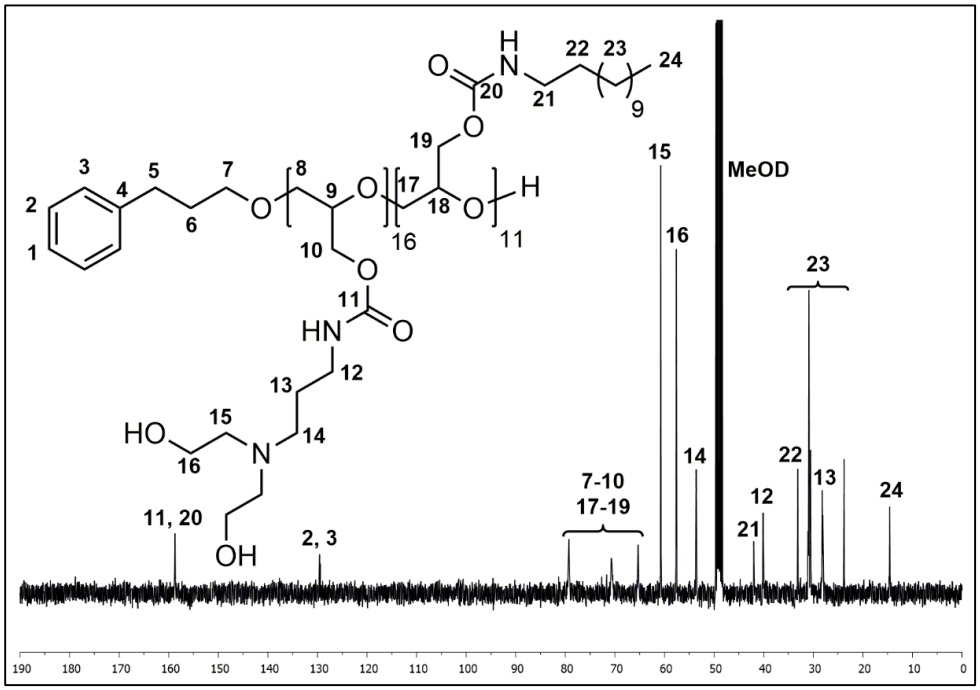

Figure S11. ^{13}C NMR spectrum of P(G$^{APDEA}_{16}$-*co*-G$^{DDA}_{11}$) (**4**) measured in MeOD.

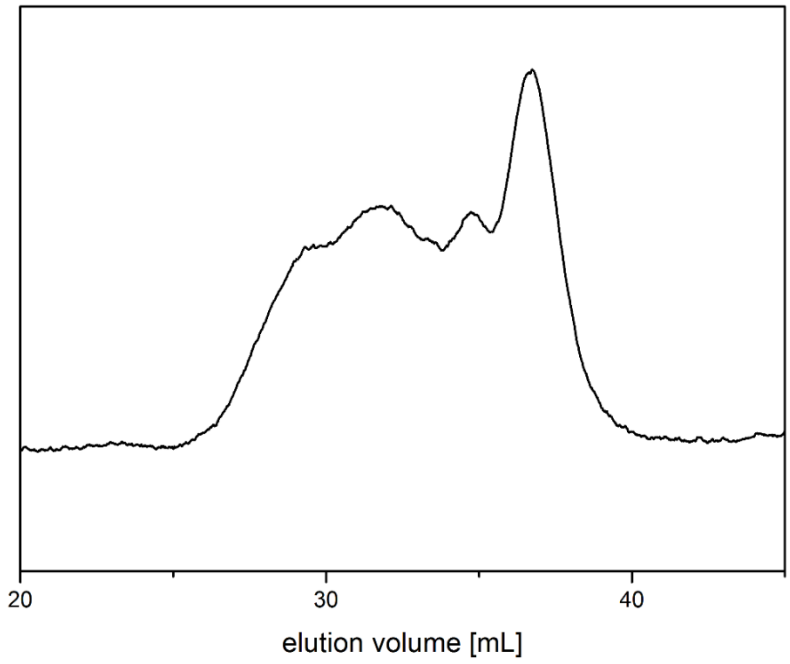

Figure S12. DMF-SEC traces of P(G^{APDEA}_{16}-*co*-G^{DDA}_{11}) (**4**).

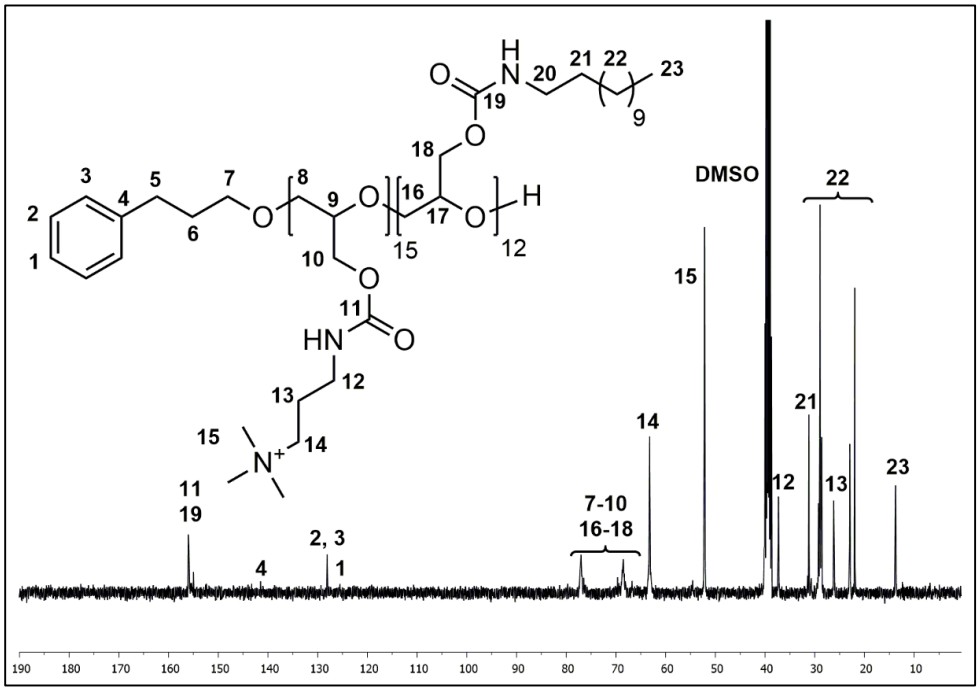

Figure S13. ^{13}C NMR spectrum of P(G^{TMAPA}_{15}-*co*-G^{DDA}_{12}) (**5**) measured in DMSO-d_6.

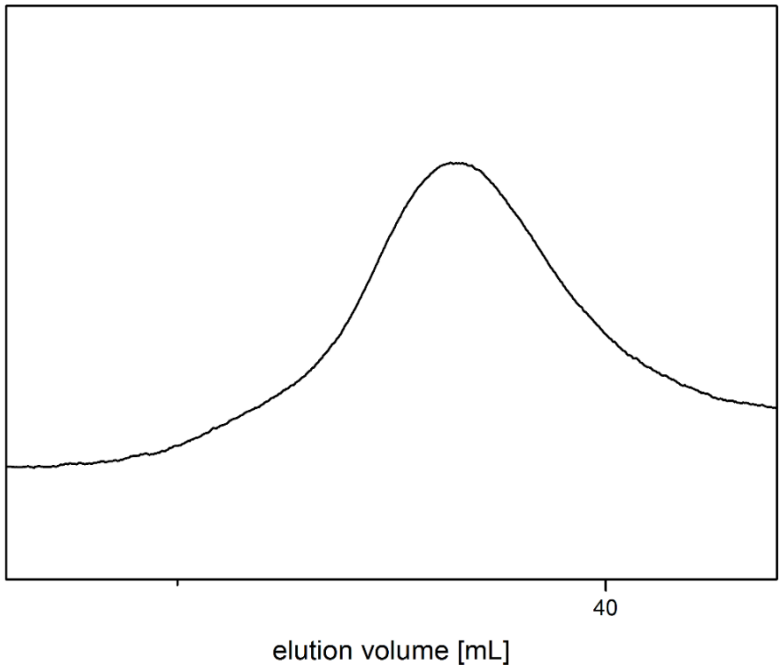

Figure S14. DMF-SEC traces of P(G^{TMAPA}_{15}-*co*-G^{DDA}_{12}) (**5**).

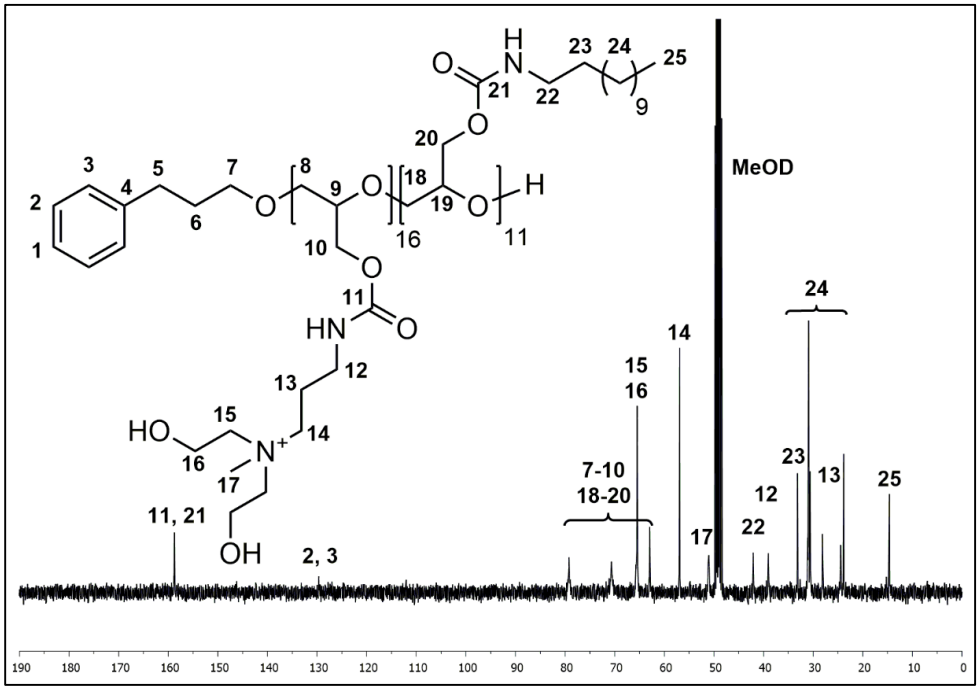

Figure S15. ^{13}C NMR spectrum of P(G^{APDEMA}_{16}-*co*-G^{DDA}_{11}) (**6**) measured in MeOD.

4. Synthesis of $P(G^{DDAc,\ q})_{27}$ (10)

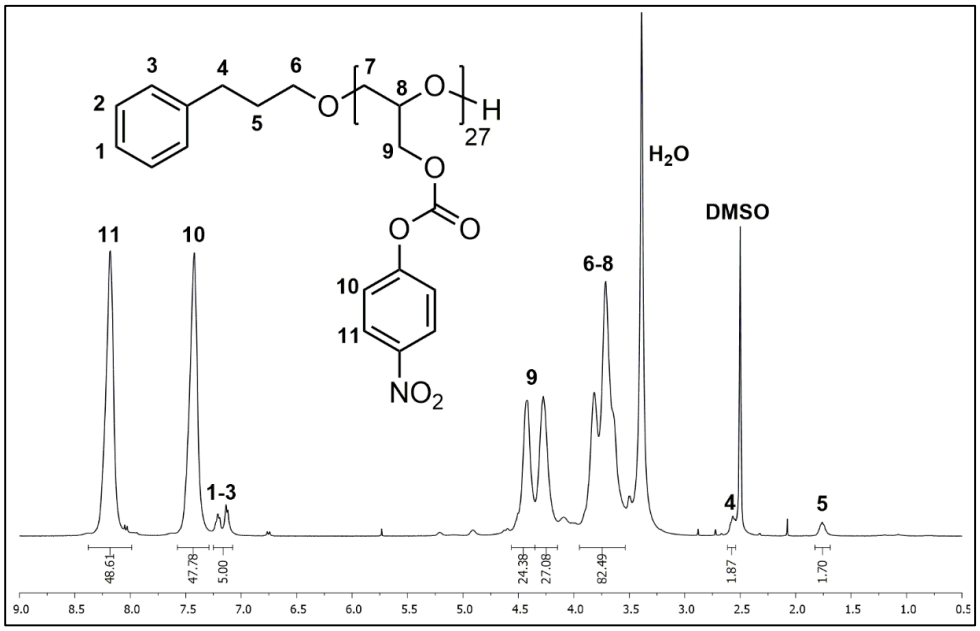

Figure S16. ^{1}H NMR spectrum of $P(G^{NPC})_{27}$ (**7**) measured in DMSO-d_6.

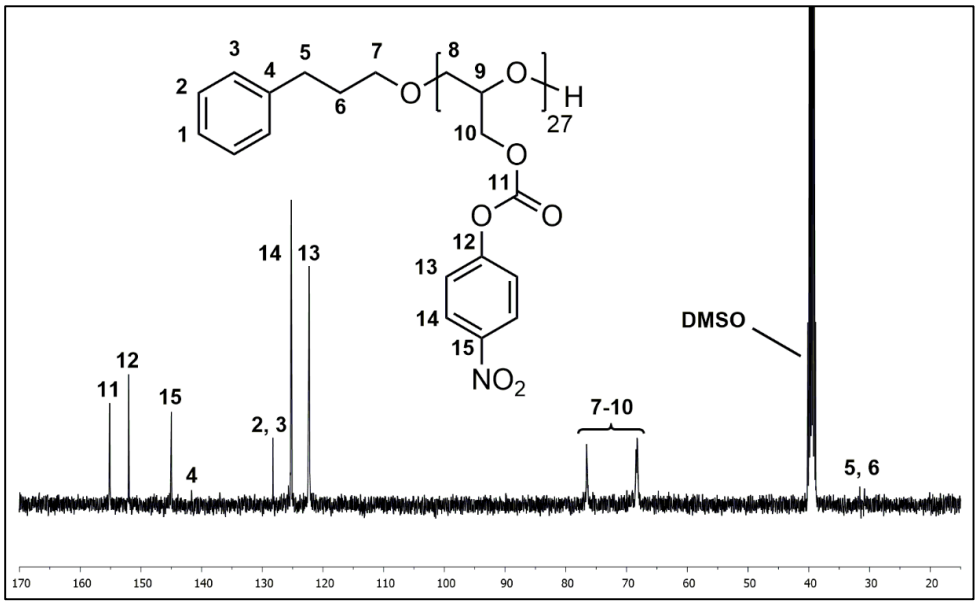

Figure S17. ^{13}C NMR spectrum of $P(G^{NPC})_{27}$ (**7**) measured in DMSO-d_6.

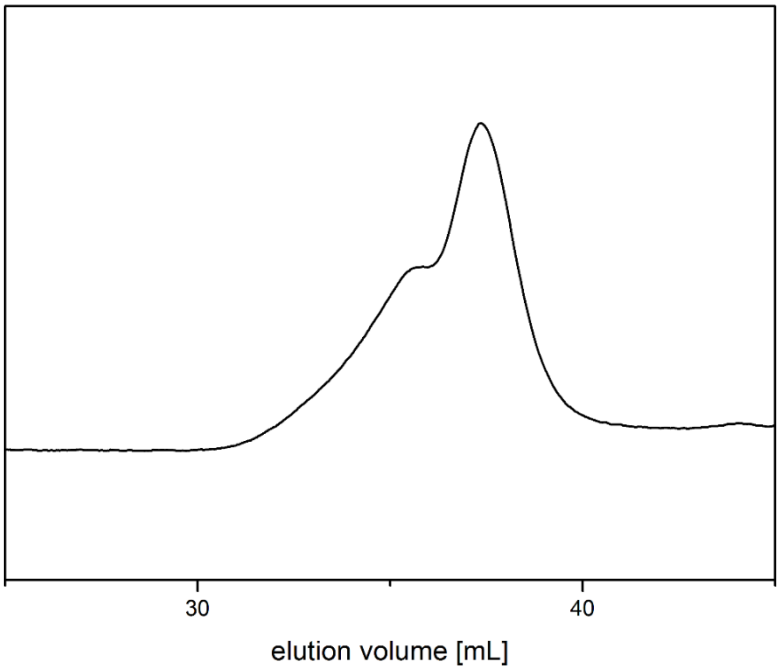

Figure S18. DMF-SEC traces of P(G^{NPC})$_{27}$ (**7**).

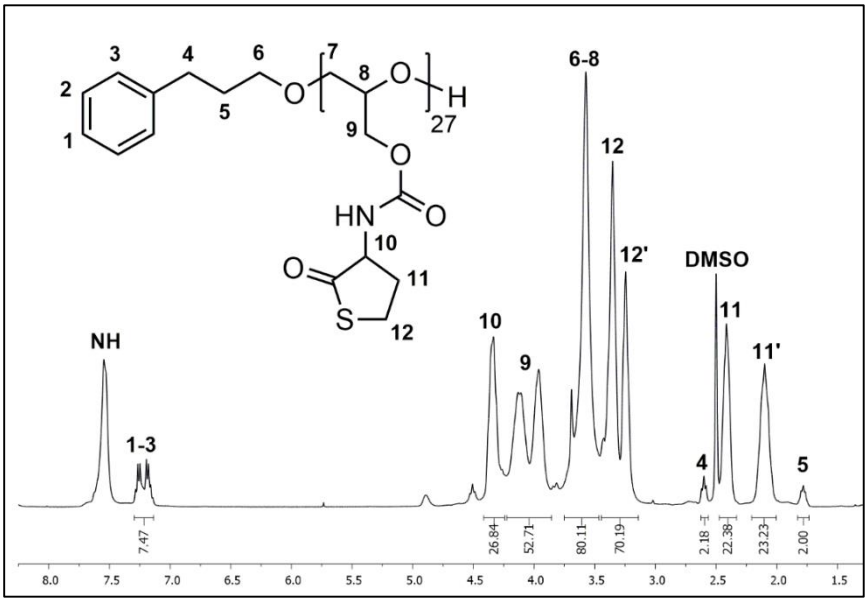

Figure S19. ^{1}H NMR spectrum of P(G^{HCTL})$_{27}$ (**8**) measured in DMSO-d_6.

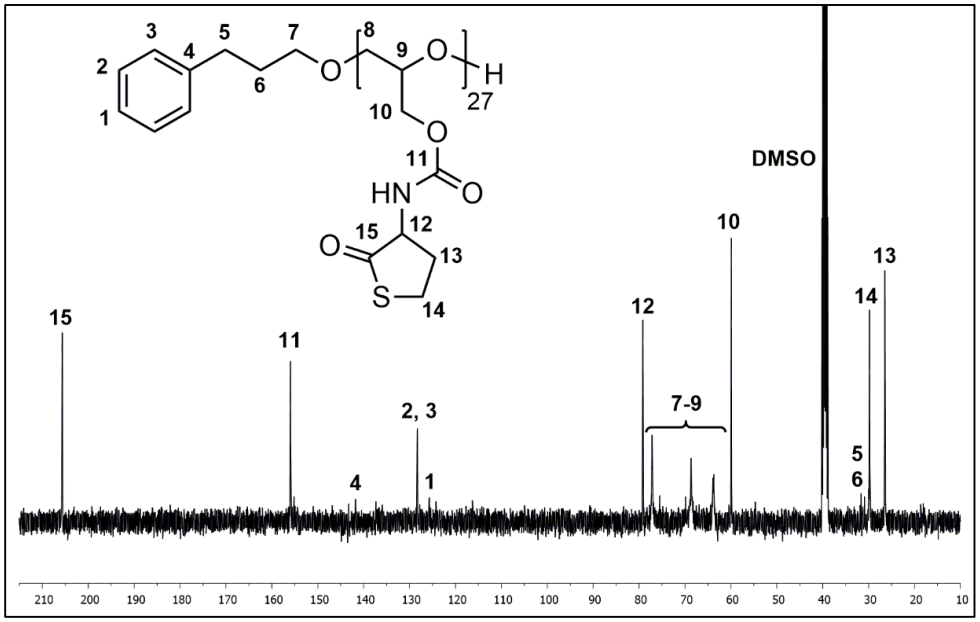

Figure S20. ^{13}C NMR spectrum of P(G^{HCTL})$_{27}$ (**8**) measured in DMSO-*d*$_6$.

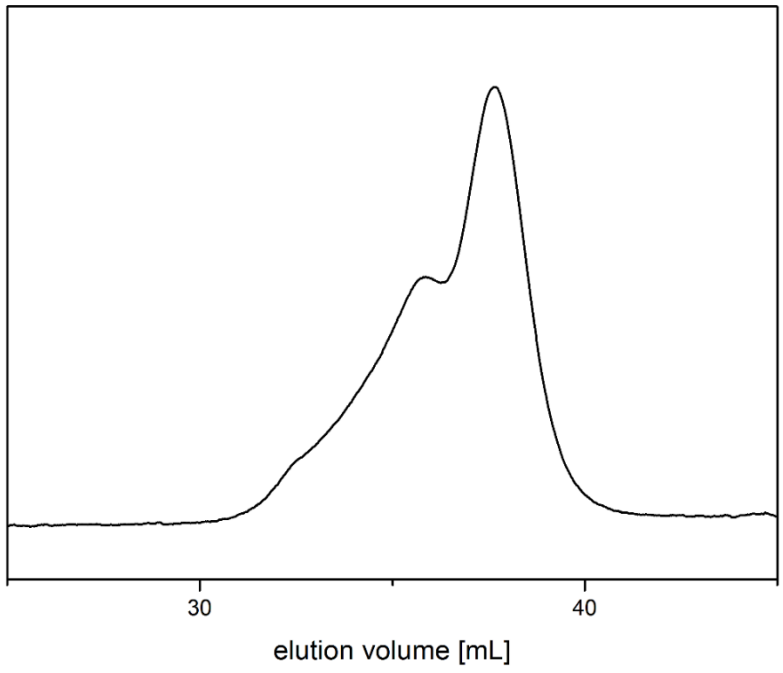

Figure S21. DMF-SEC traces of P(G^{HCTL})$_{27}$ (**8**).

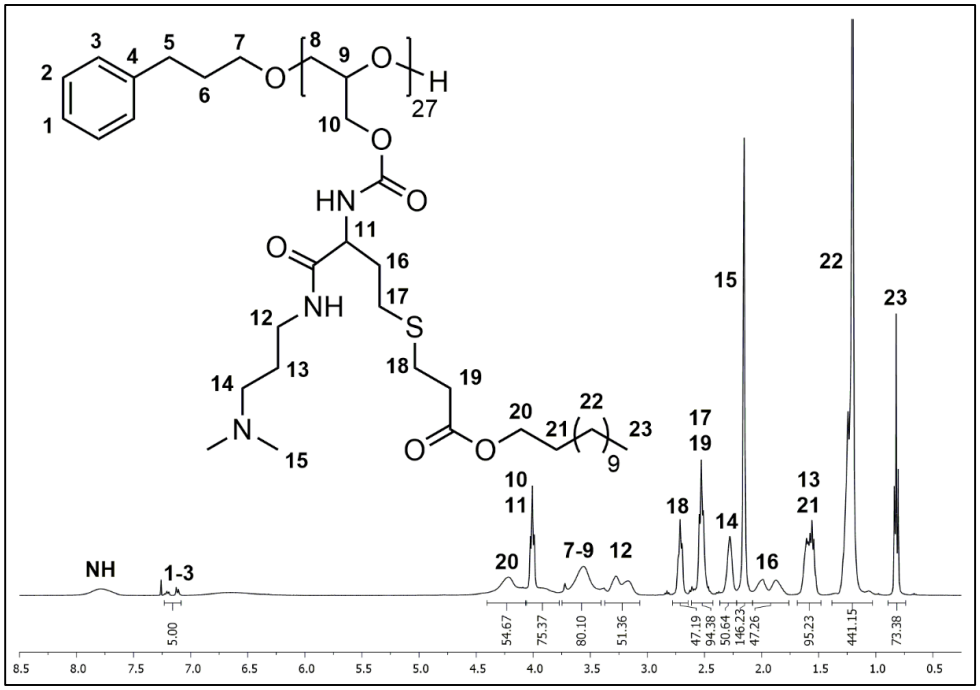

Figure S22. ^{1}H NMR spectrum of P(G^{DDAc})$_{27}$ (**9**) measured in CDCl$_3$.

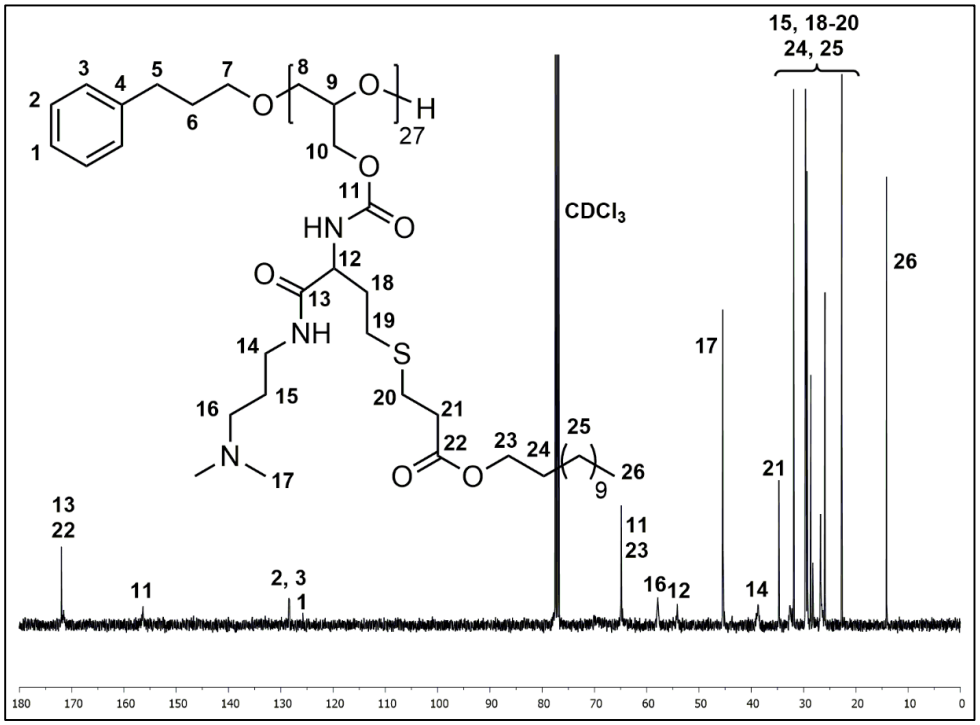

Figure S23. ^{13}C NMR spectrum of P(G^{DDAc})$_{27}$ (**9**) measured in CDCl$_3$.

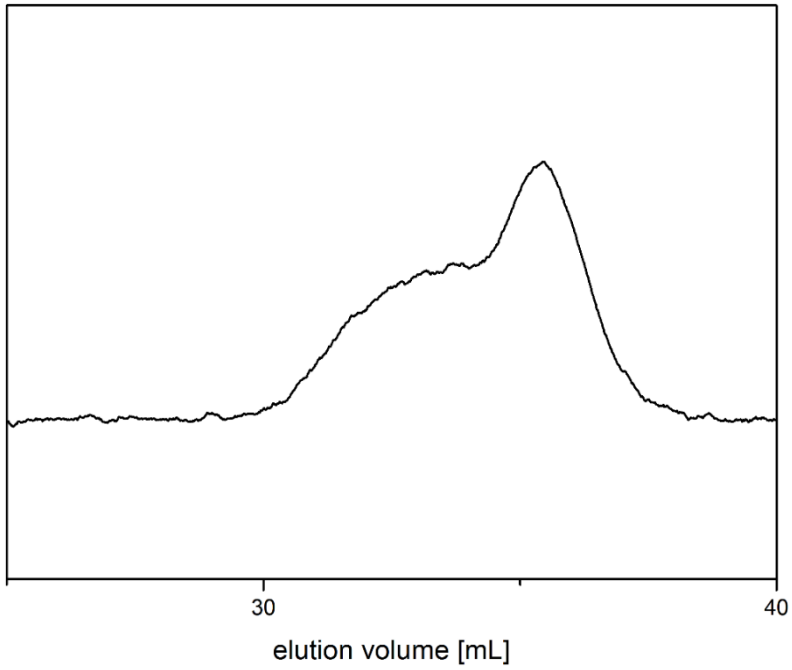

Figure S24. DMF-SEC traces of P(G^{DDAc})$_{27}$ (**9**).

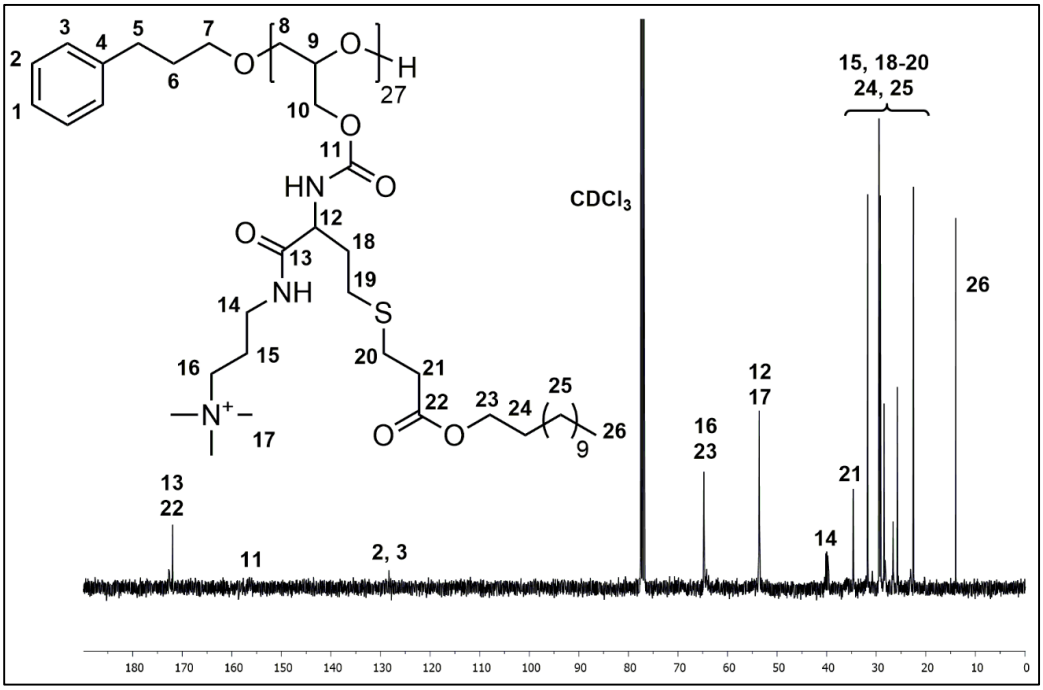

Figure S25. ^{13}C NMR spectrum of P($G^{DDAc,\ q}$)$_{27}$ (**10**) measured in $CDCl_3$.

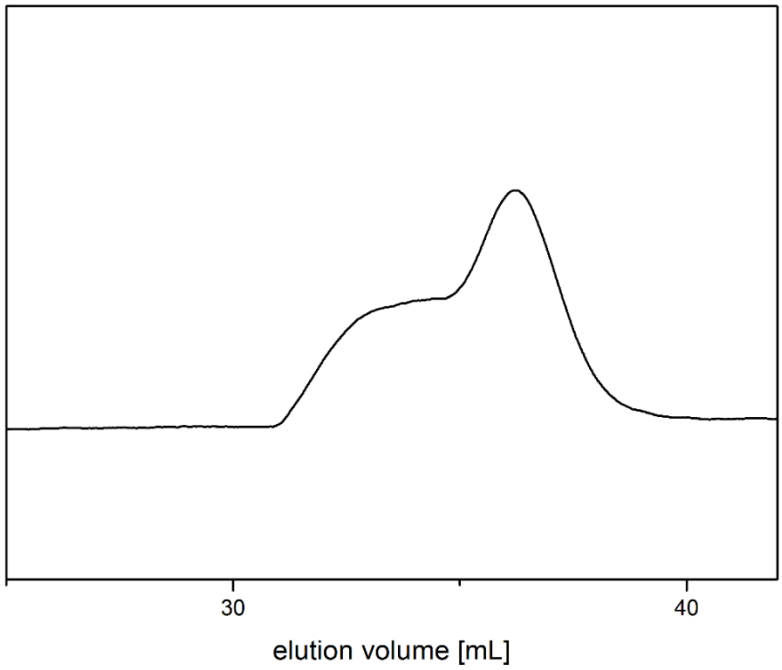

Figure S26. DMF-SEC traces of P($G^{DDAc, q}$)$_{27}$ (**10**).

5. Synthesis of P(G^{TMAPA}_{14}-*co*-$G^{DDADDAc}_{13}$) (12)

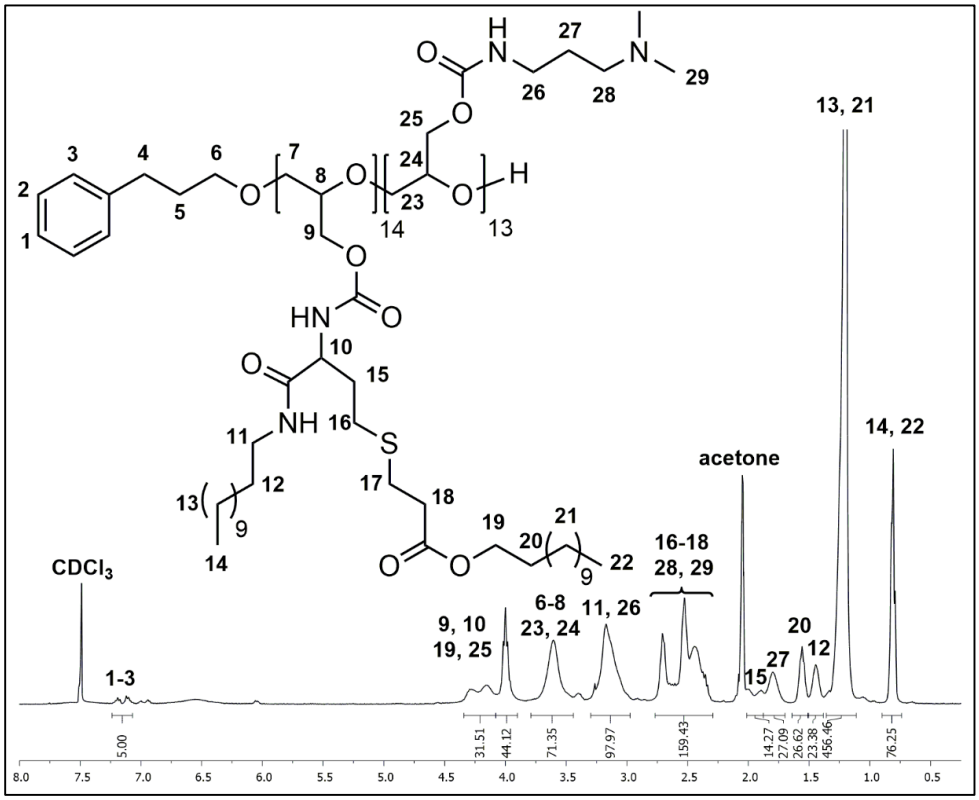

Figure S27. ^{1}H NMR spectrum of P(G^{DMAPA}_{14}-*co*-$G^{DDADDAc}_{13}$) (**11**) measured in $CDCl_3$/acetone-d_6.

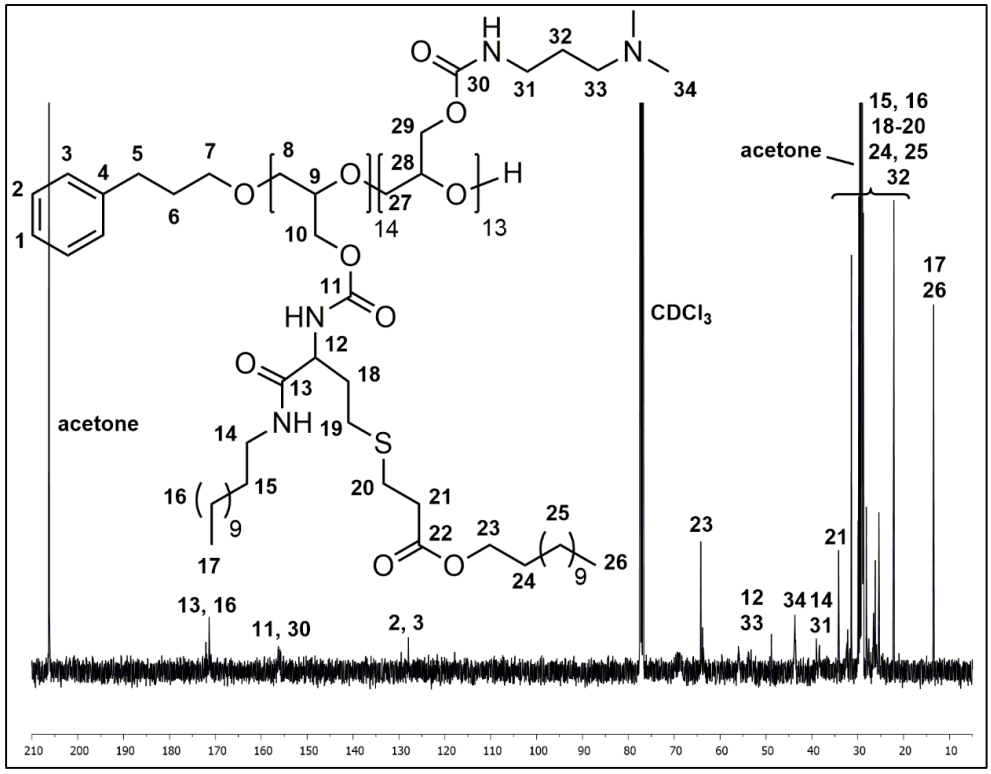

Figure S28. ^{13}C NMR spectrum of P(G$^{DMAPA}_{14}$-*co*-G$^{DDADDAc}_{13}$) (**11**) measured in $CDCl_3$/acetone-d_6.

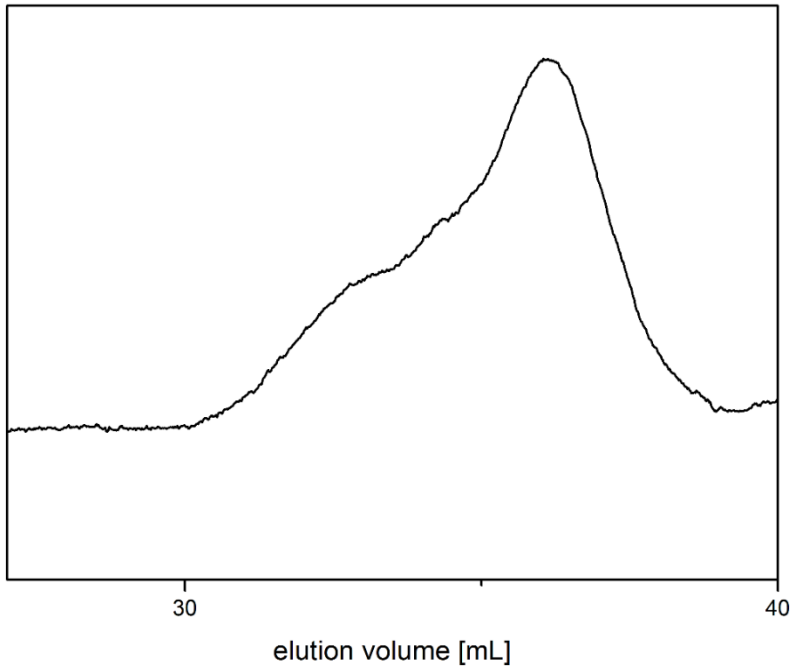

Figure S29. DMF-SEC traces of P(G$^{DMAPA}_{14}$-*co*-G$^{DDADDAc}_{13}$) (**11**).

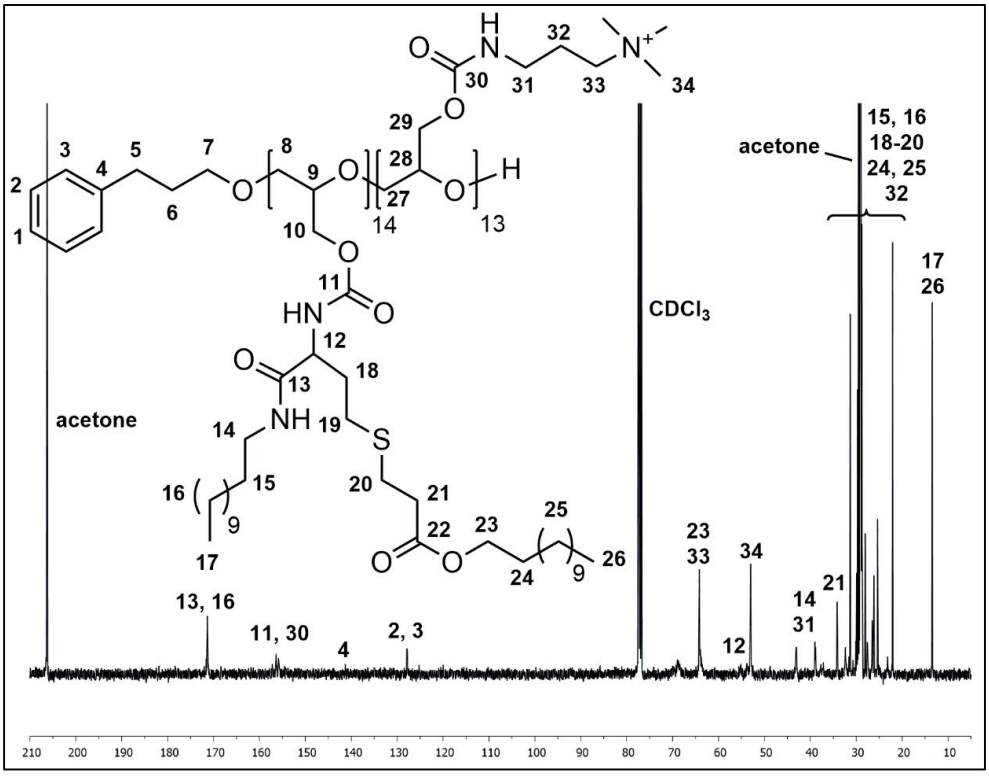

Figure S30. ^{13}C NMR spectrum of P(G^{TMAPA}_{14}-*co*-$G^{DDADDAc}_{13}$) (**12**) measured in $CDCl_3$/acetone-d_6.

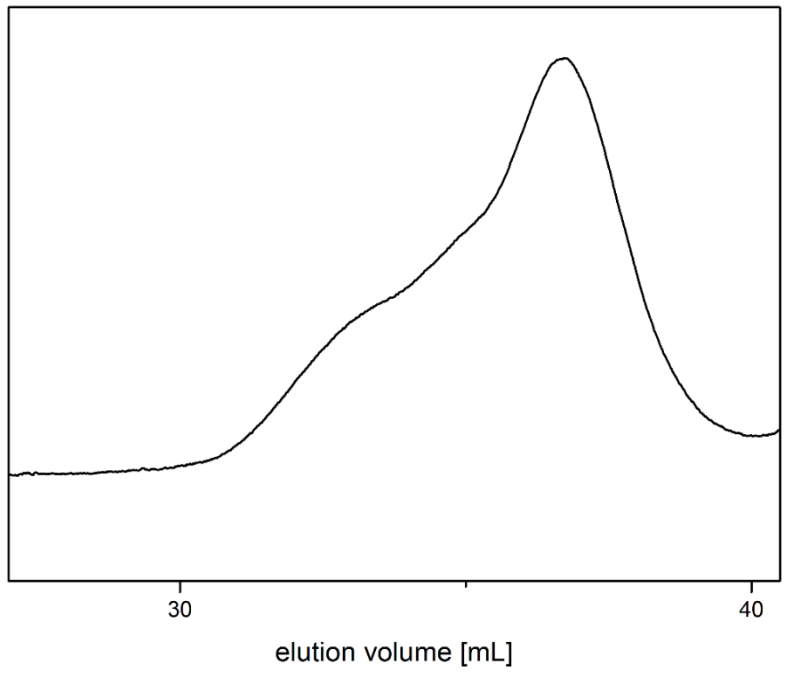

Figure S31. DMF-SEC traces of P(G^{TMAPA}_{14}-*co*-$G^{DDADDAc}_{13}$) (**12**).